JACS
JOURNAL OF THE AMERICAN CHEMICAL SOCIETY
Communication
pubs.acs.org/JACS

Level Alignment of a Prototypical Photocatalytic System: Methanol on TiO_2(110)

Annapaola Migani,*[,†,‡] Duncan J. Mowbray,*[,†] Amilcare Iacomino,[†] Jin Zhao,[§] Hrvoje Petek,[∥] and Angel Rubio*[,†]

[†]Nano-Bio Spectroscopy Group and ETSF Scientific Development Center, Departamento de Física de Materiales, Centro de Física de Materiales CSIC-UPV/EHU-MPC and DIPC, Universidad del País Vasco UPV/EHU, E-20018 San Sebastián, Spain

[‡]Consejo Superior de Investigaciones Cientificas (CSIC), ICN2 Building, E-08193 Bellaterra (Barcelona), Spain

[§]Physics Department, Hefei National Laboratory for Physical Sciences at Microscale, University of Science and Technology of China, Hefei, Anhui 230026, China

[∥]Department of Physics and Astronomy, University of Pittsburgh, Pittsburgh, Pennsylvania 15260, United States

Supporting Information

ABSTRACT: Photocatalytic activity depends on the optimal alignment of electronic levels at the molecule−semiconductor interface. Establishing the level alignment experimentally is complicated by the uncertain chemical identity of the surface species. We address the assignment of the occupied and empty electronic levels for the prototypical photocatalytic system consisting of methanol on a rutile TiO_2(110) surface. Using many-body quasiparticle (QP) techniques, we show that the frontier levels measured in UV photoelectron and two-photon photoemission spectroscopy experiments can be assigned to molecularly chemisorbed methanol rather than its dissociated product, the methoxy species. We find that the highest occupied molecular orbital of the methoxy species is much closer to the valence band maximum, suggesting why it is more photocatalytically active than the methanol molecule. We develop a general semiquantitative model for predicting many-body QP energies based on the electronic screening within the bulk, molecular, or vacuum regions of the wave functions at molecule−semiconductor interfaces.

Molecular energy levels are strongly renormalized when molecules are brought into contact with surfaces.[1] The energy positions of the frontier highest occupied molecular orbital (HOMO) and lowest unoccupied molecular orbital (LUMO) of the adsorbate with respect to the valence band maximum (VBM) and conduction band minimum (CBM) of the photocatalytic substrate define the potentials for electron transfer across a molecule−semiconductor interface. Photoelectron spectroscopy can accurately determine the alignment of the frontier orbitals of the adsorbate with respect to the substrate bands if the chemical state of the chemisorbed molecule is known. The chemical assignment and correct description of the molecule−photocatalyst interaction require theory to accurately predict the electronic structure of the coupled system.

We consider the electronic structure of methanol chemisorbed intact or in its partially dissociated methoxy form on the stoichiometric rutile TiO_2(110) surface. Experimentally, the electronic structure and photocatalytic activity of methanol on the single-crystal rutile TiO_2(110) surface under ultrahigh vacuum (UHV) conditions have been investigated by UV, X-ray, and two-photon photoelectron spectroscopies (UPS, XPS, and 2PP, respectively),[2−5] scanning tunneling microscopy (STM),[5−7] and mass spectrometric analysis of reaction products.[8,9] These experiments have reached contradictory conclusions regarding whether the empty "Wet electron" level[10] that is observed in 2PP spectra of methanol-covered TiO_2 surfaces should be assigned to the methanol or methoxy species.[4,5] Furthermore, although it is clear that the methoxy species is more photocatalytically active than the methanol molecule, there is still debate as to whether the decomposition of methanol to formaldehyde and methyl formate is initiated by the thermal[7,8] or photocatalytic[3,5,9] decomposition of methanol.

As the molecule approaches the substrate, the mutual polarization of their charge distributions (i.e., screening) renormalizes the molecular energy levels. A proper treatment of the inhomogeneous screening by the environment requires the use of many-body quasiparticle (QP) techniques.[11] We carried out many-body QP calculations at the G_0W_0 level and with the *scGW*1 self-consistent approach described in the Supporting Information (SI).[12] These are based on DFT calculations using a generalized gradient approximation to the exchange−correlation (xc) functional (PBE).[13] We also performed self-consistent QP calculations at the *scGW* and $scGW_0$ levels and DFT calculations using a hybrid xc functional (HSE).[14] PBE, HSE, *scGW*, and $scGW_0$ calculations all failed to describe even qualitatively the level alignment of methanol on TiO_2(110) (see the SI). However, from G_0W_0 and *scGW*1 calculations we obtained the correct level alignment for both the occupied and empty molecular levels at the interface. This enabled us to conclude that the molecular structures measured in UPS[2] and 2PP[15] experiments can mostly be attributed to intact methanol molecules on TiO_2(110). For the partially dissociated methanol layer we found that the HOMO of the methoxy species is nearer the VBM. This more favorable HOMO alignment may explain why the methoxy species is more photocatalytically active

Received: April 13, 2013
Published: July 18, 2013

   dx.doi.org/10.1021/ja4036994 | *J. Am. Chem. Soc.* 2013, 135, 11429−11432

than the methanol molecule. Of more general significance, we found that the many-body QP corrections to the DFT energy levels (i.e., the G_0W_0 QP energy shifts) are correlated quantitatively with the fractions of the levels' densities within the bulk, molecular, and vacuum regions. This enabled us to construct a model that quantitatively describes the QP corrections to the electronic energy levels at a molecule−semiconductor interface.

The adsorption of methanol on rutile TiO_2(110) is highly inhomogeneous because of the similarity of the energies of several configurations. Methanol can chemisorb intact through its O atom to a coordinately unsaturated (cus) Ti site of the substrate or by H-bonding between the H atom of its OH group and the surface bridging O atom. It can also dissociate by transferring the H atom to the surface through the H-bond, leaving a methoxy species at the cus Ti site. The degree of dissociation and whether it occurs thermally or photocatalytically are unknown. The relative stabilities and structures of intact, 50% dissociated, and 100% dissociated methanol monolayers were calculated in ref 16. We performed G_0W_0 QP calculations of the interfacial electronic structures of the four most stable methanol monolayers (Figure 1), which include two "intact" methanol

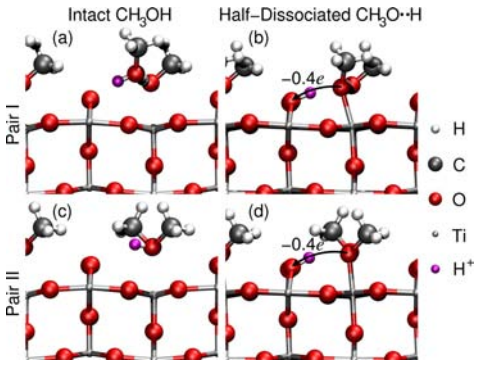

Figure 1. Atomic structure of methanol monolayers on TiO_2(110). Geometries for (a, c) intact and (b, d) half-dissociated (a, b) pair I and (c, d) pair II monolayers are shown. The transfer of a proton (marked in magenta) is accompanied by a CT of 0.4 electron.

monolayers and their "half-dissociated" counterparts. In these structures, half of the methanol molecules have an intermolecular H-bond while the other half have an interfacial H-bond. Proton transfer and an accompanying charge transfer (CT) of 0.4 electron from the methanol oxygen to the nearest surface bridging oxygen occur through this interfacial H-bond.

Bridging oxygen vacancies, substoichiometricity of the bulk, and interstitial Ti atoms were not taken into account in these models. Nevertheless, the simulated and measured XPS[3] C 1s (−0.66 vs −0.6 eV) and O 1s (−1.94 vs −1.7 eV) core-level shifts were in semiquantitative agreement for the most stable intact methanol monolayer and its half-dissociated counterpart (pair I). This demonstrates that these structures are realistic models for UHV experiments. Here we focused on the "initial state" electronic structure of the interface prior to photon irradiation under UHV conditions, as the HOMO level alignment may change upon creation of a hole or the presence of solvent.[17]

Figure 2 shows the electronic structure for pair I. First, we focused on the highest-energy peak in the UPS spectrum at $\epsilon_{peak}^{UPS} \approx -1.55$ eV relative to the VBM (ϵ_{VBM}). By comparing the projected density of states (PDOS) onto the methanol layer with UPS measurements[2] of CH_3OH/TiO_2 in Figure 2a, we found the

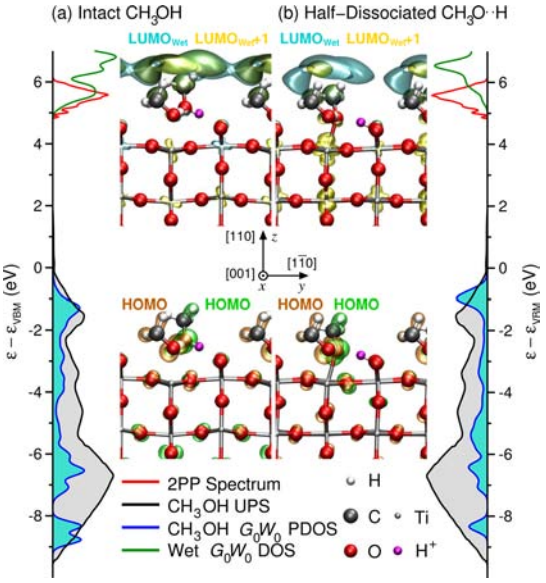

Figure 2. Electronic structures of methanol monolayers on TiO_2(110). CH_3OH projected and Wet DOS computed with G_0W_0 for the depicted (a) intact and (b) half-dissociated pair I structures are compared with the UPS[2] and 2PP[15] spectra. Filling denotes occupied levels. Energies are relative to the VBM (ϵ_{VBM}). The H atom undergoing proton transfer is marked in magenta. The HOMO for the deprotonating methanol molecule and the methanol molecule H-bonded to it are shown together below, with the $LUMO_{Wet}$ and $LUMO_{Wet}$+1 above.

corresponding peak to be in semiquantitative agreement with the intact structure, which is ca. 0.3 eV closer to the VBM. This PDOS feature corresponds to distinct HOMOs localized on each methanol molecule within the unit cell, as depicted in green or orange in Figure 2. These are predominantly nonbonding O 2p orbitals, with some C−H σ and Ti 3d character. The weak hybridization of the HOMO orbitals with the substrate is reflected in the relative narrowness of the primary peaks. The PDOS for the half-dissociated structure (Figure 2b) is shifted ca. 0.6 eV closer to the VBM than the UPS data. The comparison with UPS experiments suggests that it is mostly the intact methanol layer that is measured at ca. 298 K.[2]

Turning to the unoccupied molecular levels in Figure 2, we found that they have primarily two-dimensional (2D) σ* character associated with the methanol C−H bond, with weight above H atoms outside the molecular layer.[4] These are the "Wet electron" levels,[10] which give an intense experimental peak in the 2PP spectra at $\epsilon_{peak}^{2PP} \approx 5.58$ eV.[15] The Wet electron DOS (Wet DOS) at the G_0W_0 level is also in better agreement with experiment for the intact structure than for the half-dissociated one, as is evident in Figure 2. The $LUMO_{Wet}$ and $LUMO_{Wet}$+1 levels, which are located at the onset of the Wet DOS spectrum, are shown in Figure 2.

Our G_0W_0 results favor the assignment of both the UPS and 2PP measurements to the intact methanol overlayers ($\Delta\epsilon^{UPS} \approx +0.26$ eV, $\Delta\epsilon^{2PP} \approx +0.10$ eV; Table S1 in the SI). This is fully supported by the PDOS and Wet DOS for the intact and half-dissociated structures of pair II.[16] Compared with pair I, the molecule−surface H bond is weakened and the two methyl groups are reoriented away from each other for pair II (Figure 1). The two intact structures have similar PDOS and Wet DOS peak energies (Table S1). The correspondence is even closer for the two half-dissociated structures. Overall, the shape of the spectra are quite similar in both cases. This means that the spectral

dx.doi.org/10.1021/ja4036994 | J. Am. Chem. Soc. 2013, 135, 11429−11432

assignment to intact rather than half-dissociated structures is robust against such differences in orientation within the molecular overlayer.

To quantify the influence of the screening on the vacuum level and wave functions, we had to go beyond G_0W_0 to the self-consistent *GW* level. To maintain the accurate G_0W_0 description of the spectra while also describing the vacuum level and QP wave functions via the self-consistent *GW* procedure, we introduced the *scGW*1 approach (see the SI). In *scGW*1, the self-consistent procedure is halted once a full unit of the self-energy has been included (i.e., the xc potential is entirely replaced by self-energy). For this reason, the QP energy shifts are quite similar to those obtained using G_0W_0. Since the wave functions converge sooner than the energies within self-consistent *GW*, the QP wave functions and vacuum level are also obtained within this procedure. Indeed, the *scGW*1 spectra (Figure 3) are in even better agreement with the UPS and 2PP measurements ($\Delta\varepsilon^{UPS} \approx -0.15$ eV, $\Delta\varepsilon^{2PP} \approx +0.04$ eV; Table S1) than the G_0W_0 ones.

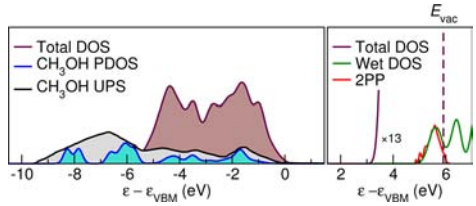

Figure 3. Total, CH_3OH projected, and Wet DOS computed with *scGW*1 for the intact structure of pair I. The calculated CH_3OH PDOS and Wet DOS are compared with the UPS[2] and 2PP[15] spectra. Filling denotes occupied levels. Energies are relative to ε_{VBM}. The dashed vertical line indicates the vacuum level (E_{vac}).

To better understand the differences between G_0W_0 and *scGW*1 for the CH_3OH PDOS and Wet DOS shown in Figures 2a and 3, we considered the Kohn–Sham and QP HOMO and $LUMO_{Wet}$ wave functions depicted in Figure 4. We found that

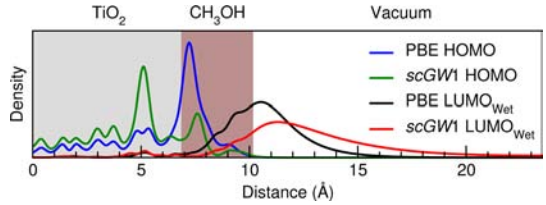

Figure 4. HOMO and $LUMO_{Wet}$ average densities in the *xy* plane vs distance from the center of the TiO_2 substrate at Γ as obtained from PBE and *scGW*1. The TiO_2 bulk, CH_3OH molecular layer, and vacuum are depicted as gray, brown, and white regions, respectively.

the $LUMO_{Wet}$ level changes from being a molecular level with σ^* character in PBE to a more delocalized image-potential-like level in *scGW*1, as found previously for insulator surfaces.[18] Just as the $LUMO_{Wet}$ level becomes more delocalized at the QP level, the HOMO becomes more hybridized with the threefold-coordinated oxygen atoms at the surface. In fact, the screening is qualitatively different for molecular and bulk occupied levels. This leads to a strong dependence of the QP energy corrections on the character of the occupied level.

To determine the chemical origin of the QP energy corrections, we determined how the shifts correlate with the bulk, molecular, and vacuum characters of the wave function (Figure 5). To quantify the wave function's character, we

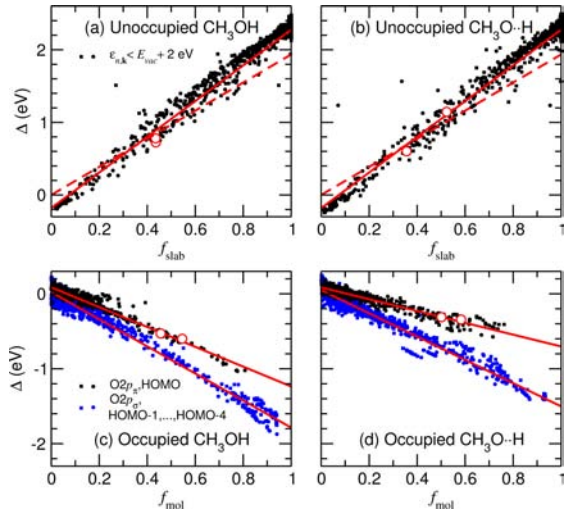

Figure 5. G_0W_0 QP energy correction (Δ) vs (a, b) the fraction of the wave function's density in in the slab (f_{slab}) for the unoccupied levels and (c, d) the fraction in the molecular layer (f_{mol}) for the occupied levels for the (a, c) intact and (b, d) half-dissociated structures of pairs I (●) and II (■). Open circles denote the (a, b) $LUMO_{Wet}$ and $LUMO_{Wet}$+1 and (c, d) HOMO at Γ depicted in Figure 2. Red solid lines are linear fits. Dashed lines denote $\Delta \approx \Delta_{bulk} f_{slab}$.

designated the bulk, molecular, and vacuum regions and calculated the fraction of the wave function's surface-averaged density in each, as shown in Figure 4. At the G_0W_0 level, the QP energy shift (Δ) is the difference between the QP self-energy (Σ) and the xc potential (V_{xc}) normalized by a factor *Z* for a particular level [i.e., $\Delta \equiv Z(\Sigma - V_{xc})$].[12] We found that the QP shift for each unoccupied level is correlated with the weight on the slab (f_{slab}), which corresponds to the sum of the weights in the bulk and molecular regions. The same correlation with f_{slab} was obtained for the unoccupied levels of the two intact and two half-dissociated structures (Figure 5a,b, respectively). This indicates that the magnitude of the QP shift is determined by the fraction of the wave function that is not in the vacuum.

Indeed, vacuum or free electron levels are reasonably well described by DFT. This means that the QP corrections are rather small, as the self-energies of these levels are well-described by their xc potentials (i.e., $\Sigma \approx V_{xc}$). Because the Wet electron levels have a large weight in the vacuum, their QP corrections ($0.6 \text{ eV} \lesssim \Delta \lesssim 1.2$ eV) are intermediate between those for the bulk level ($\Delta_{slab} \approx 2.28$ eV) and the vacuum level ($\Delta_{vac} \approx -0.18$ eV). From this we obtain the relation $\Delta \approx \Delta_{vac} + (\Delta_{slab} - \Delta_{vac}) f_{slab}$ for the QP energy shift.

The QP corrections for the $LUMO_{Wet}$ and $LUMO_{Wet}$+1 levels at Γ (depicted in Figure 2) are shown as open circles in Figure 5a,b. For the half-dissociated geometry in Figure 2b, the $LUMO_{Wet}$+1 level is significantly more hybridized with the bulk compared with the $LUMO_{Wet}$ level as well as the $LUMO_{Wet}$ and $LUMO_{Wet}$+1 levels of the intact structure in Figure 2a. As a consequence, the $LUMO_{Wet}$+1 level of the half-dissociated structure has a significantly larger QP shift (Figure 5b).

We may justify the correlation between Δ and f_{slab} using the following simple physical model. First, because $\Sigma \approx V_{xc}$ for the vacuum and nearly free electron levels, $\Delta_{vac} \approx 0$. Second, because the QP energy shifts within the slab are dominated by those of the bulk, Δ_{slab} can be approximated by the calculated QP shifts for the bulk TiO_2 unoccupied levels (i.e., $\Delta_{slab} \approx \Delta_{bulk} \approx 1.93$ eV). From this we obtain the linear correlation $\Delta \approx \Delta_{bulk} f_{slab}$ with a

dx.doi.org/10.1021/ja4036994 | J. Am. Chem. Soc. 2013, 135, 11429–11432

standard deviation of $\sigma \approx \pm 0.2$ eV with respect to the full calculation (dashed lines in Figure 5a,b). These results suggest that f_{slab} may serve as an effective descriptor for the QP energy shifts of the unoccupied levels at the interface.

In contrast, we found the QP shifts for the occupied levels to be well-correlated with the fraction of the wave function's density within the molecular layer (f_{mol}), as was the case for a NaCl insulating film on Ge(001).[19] This means that screening within the molecular layer plays an important role for the occupied levels. The correlation is specific to the type of molecular layer (i.e., intact versus half-dissociated). Furthermore, we found that the correlation is also orbital-dependent, with separate correlations for the weakly bonding O $2p_\pi$ and HOMO and the more strongly hybridized O $2p_\sigma$ and HOMO−1 through HOMO−4. This is because it is easier to screen σ orbitals, which are located between the atoms, than π orbitals, which are out of plane. The O $2p_\pi$ and O $2p_\sigma$ orbitals are labeled according to ref 20, while HOMO−1 through HOMO−4 include the corresponding levels for each type of methanol. The first set of levels includes the VBM and all levels close to the VBM in energy. For this reason, it is the relevant set of levels for hole trapping at the geometry of the unexcited methanol layer prior to photon irradiation. For the O $2p_\pi$ orbitals, focusing on the HOMO levels depicted in Figure 2, we found a larger QP shift for the intact layer (ca. −1.2 eV; Figure 5c) than the half-dissociated layer (ca. −0.7 eV; Figure 5d), while bulk levels are essentially unshifted.

The observed differences in the QP shifts are due to changes in the screening, as V_{xc} is almost the same for the HOMOs of the intact and half-dissociated methanol overlayers. These differences in screening are related to the proton-associated CT of 0.4 electron for pairs I and II (Figure 1). When charge is transferred out of the monolayer, its ability to screen electrons is reduced. Further, the O $2p_\pi$ and HOMO levels are more strongly affected by CT than the σ levels, as they are more easily polarized. This CT dependence is the origin of the destabilization of the HOMO for the half-dissociated versus intact structures, which may explain the measured differences in photocatalytic activity. Such a destabilization of the HOMO has previously been observed by UPS for catechol on TiO_2(110).[21] The same set of correlations hold for each type of structure from pairs I and II. Altogether, this means that f_{mol} is an appropriate descriptor for the QP energy shifts of the occupied levels at the interface.

Overall, we found that the screening of the occupied levels is affected by CT (intact $\gtrsim$ dissociated) and the spatial distribution of the wave function ($\sigma \gtrsim \pi$). For the unoccupied levels, we found that the correlation is independent of CT because these levels are highly delocalized, so minor changes in the local screening due to CT are "washed out" by the larger differences in screening between the vacuum and slab regions.

In this work, many-body QP techniques have provided fundamental insight into the underlying processes that control the level alignment of methanol on TiO_2(110). This is a major advancement in the accurate prediction of interfacial level alignment, which is of fundamental importance in photocatalysis.

■ ASSOCIATED CONTENT

Supporting Information

Methods and additional results. This material is available free of charge via the Internet at http://pubs.acs.org.

■ AUTHOR INFORMATION

Corresponding Author

amigani@cin2.es; duncan.mowbray@gmail.com; arubio@ehu.es

Notes

The authors declare no competing financial interest.

■ ACKNOWLEDGMENTS

We acknowledge funding from the European Projects DYNamo (ERC-2010-AdG-267374) and CRONOS (280879-2 CRONOS CP-FP7), Spanish Grants (FIS2010-21282-C02-01, PIB2010US-00652, RYC-2011-09582, JAE DOC, and JCI-2010-08156), Grupos Consolidados UPV/EHU del Gobierno Vasco (IT-319-07), NNSFC (21003113 and 21121003), MOST (2011CB921404), and NSF (CHE-1213189) and computational time from i2basque, BSC Red Espanola de Supercomputacion, and EMSL at PNNL (DOE).

■ REFERENCES

(1) (a) Neaton, J. B.; Hybertsen, M. S.; Louie, S. G. *Phys. Rev. Lett.* **2006**, *97*, No. 216405. (b) Garcia-Lastra, J. M.; Rostgaard, C.; Rubio, A.; Thygesen, K. S. *Phys. Rev. B* **2009**, *80*, No. 245427.

(2) Onishi, H.; Aruga, T.; Egawa, C.; Iwasawa, Y. *Surf. Sci.* **1988**, *193*, 33.

(3) Yuan, Q.; Wu, Z.; Jin, Y.; Xu, L.; Xiong, F.; Ma, Y.; Huang, W. *J. Am. Chem. Soc.* **2013**, *135*, 5212.

(4) Li, B.; Zhao, J.; Onda, K.; Jordan, K. D.; Yang, J.; Petek, H. *Science* **2006**, *311*, 1436.

(5) Zhou, C.; Ren, Z.; Tan, S.; Ma, Z.; Mao, X.; Dai, D.; Fan, H.; Yang, X.; LaRue, J.; Cooper, R.; Wodtke, A. M.; Wang, Z.; Li, Z.; Wang, B.; Yang, J.; Hou, J. *Chem. Sci.* **2010**, *1*, 575.

(6) Henderson, M. A.; Lyubinetsky, I. *Chem. Rev.* **2013**, *113*, 4428.

(7) Shen, M.; Acharya, D. P.; Dohnálek, Z.; Henderson, M. A. *J. Phys. Chem. C* **2012**, *116*, 25465.

(8) (a) Shen, M.; Henderson, M. A. *J. Phys. Chem. Lett.* **2011**, *2*, 2707. (b) Phillips, K. R.; Jensen, S. C.; Baron, M.; Li, S.-C.; Friend, C. M. *J. Am. Chem. Soc.* **2013**, *135*, 574.

(9) Guo, Q.; Xu, C.; Ren, Z.; Yang, W.; Ma, Z.; Dai, D.; Fan, H.; Minton, T. K.; Yang, X. *J. Am. Chem. Soc.* **2012**, *134*, 13366.

(10) Onda, K.; Li, B.; Zhao, J.; Jordan, K. D.; Yang, J.; Petek, H. *Science* **2005**, *308*, 1154.

(11) (a) Onida, G.; Reining, L.; Rubio, A. *Rev. Mod. Phys.* **2002**, *74*, 601. (b) Ping, Y.; Rocca, D.; Galli, G. *Chem. Soc. Rev.* **2013**, *42*, 2437. (c) Patrick, C. E.; Giustino, F. *Phys. Rev. Lett.* **2012**, *109*, No. 116801.

(12) (a) Shishkin, M.; Kresse, G. *Phys. Rev. B* **2006**, *74*, No. 035101. (b) Shishkin, M.; Kresse, G. *Phys. Rev. B* **2007**, *75*, No. 235102. (c) Shishkin, M.; Marsman, M.; Kresse, G. *Phys. Rev. Lett.* **2007**, *99*, No. 246403. (d) Caruso, F.; Rinke, P.; Ren, X.; Scheffler, M.; Rubio, A. *Phys. Rev. B* **2012**, *86*, No. 081102.

(13) Perdew, J. P.; Burke, K.; Ernzerhof, M. *Phys. Rev. Lett.* **1996**, *77*, 3865.

(14) Heyd, J.; Scuseria, G. E.; Ernzerhof, M. *J. Chem. Phys.* **2003**, *118*, 8207.

(15) Onda, K.; Li, B.; Zhao, J.; Petek, H. *Surf. Sci.* **2005**, *593*, 32.

(16) Zhao, J.; Yang, J.; Petek, H. *Phys. Rev. B* **2009**, *80*, No. 235416.

(17) Akimov, A. V.; Muckerman, J. T.; Prezhdo, O. V. *J. Am. Chem. Soc.* **2013**, *135*, 8682.

(18) Rohlfing, M.; Wang, N.-P.; Krüger, P.; Pollmann, J. *Phys. Rev. Lett.* **2003**, *91*, No. 256802.

(19) Freysoldt, C.; Rinke, P.; Scheffler, M. *Phys. Rev. Lett.* **2009**, *103*, No. 056803.

(20) Mowbray, D. J.; Martínez, J. I.; Calle-Vallejo, F.; Rossmeisl, J.; Thygesen, K. S.; Jacobsen, K. W.; Nørskov, J. K. *J. Phys. Chem. C* **2011**, *115*, 2244.

(21) Li, S.-C.; Wang, J.-g.; Jacobson, P.; Gong, X.-Q.; Selloni, A.; Diebold, U. *J. Am. Chem. Soc.* **2009**, *131*, 980.